processes

MDPI

Article

Towards the Circular Economy of Rare Earth Elements: Lanthanum Leaching from Spent FCC Catalyst by Acids

Corradino Sposato [1], Enrico Catizzone [1,*], Alessandro Blasi [1], Marilena Forte [2], Assunta Romanelli [1], Massimo Morgana [1], Giacobbe Braccio [1], Girolamo Giordano [2,3] and Massimo Migliori [2]

[1] ENEA-Italian National Agency for New Technologies, Energy and Sustainable Economic Development, Trisaia Research Centre, I-75026 Rotondella, MT, Italy; corradino.sposato@enea.it (C.S.); alessandro.blasi@enea.it (A.B.); assunta.romanelli@enea.it (A.R.); massimo.morgana@enea.it (M.M.); giacobbe.braccio@enea.it (G.B.)

[2] Laboratory of Catalysis and Industrial Chemistry, University of Calabria, Via P. Bucci, I-87036 Rende, CS, Italy; forte.marilena@libero.it (M.F.); ggiordaunical@yahoo.it (G.G.); massimo.migliori@unical.it (M.M.)

[3] European Research Institute of Catalysis, E.R.I.C. a.i.s.b.l., B-1040 Bruxelles, Belgium

* Correspondence: enrico.catizzone@enea.it; Tel.: +39-0835-974319

Abstract: Rare earth elements (REEs) are strategic materials widely used in different applications from Information and Communication Technologies (ICT) to catalysis, which are expected to grow more in the future. In order to reduce the impact of market price and reduce the environmental effect from soil extraction, recovery/purification strategies should be exploited. This paper presents a combined acid-leaching/oxalate precipitation process to recover lanthanum from spent FCC catalyst using nitric acid. Preferred to hydrochloric and sulphuric acid (preliminary assessed), HNO_3 showed a good capability to completely leach lanthanum. The combination with an oxalate precipitation step allowed demonstrating that a highly pure (>98% *w*/*w*) lanthanum solid can be recovered, with a neglectable amount of poisoning metals (Ni, V) contained into the spent catalyst. This could open a reliable industrial perspective to recover and purify REE in the view of a sustainable recycling strategy.

Keywords: rare earth elements; FCC catalyst; acid leaching; REE recycling

Citation: Sposato, C.; Catizzone, E.; Blasi, A.; Forte, M.; Romanelli, A.; Morgana, M.; Braccio, G.; Giordano, G.; Migliori, M. Towards the Circular Economy of Rare Earth Elements: Lanthanum Leaching from Spent FCC Catalyst by Acids. *Processes* **2021**, *9*, 1369. https://doi.org/10.3390/pr9081369

Academic Editor: Szabolcs Fogarasi

Received: 13 July 2021
Accepted: 3 August 2021
Published: 5 August 2021

1. Introduction

In the last decades, different chemical elements have received wide attention, due to their use in specific applications such as battery, hybrid and electric engines, energy storage, electronic devices, high-tech devices and light emitting diodes, and some of the elements are not abundant on Earth. As an example, worldwide reserves of cobalt were estimated at 6600 thousand tonnes, at the end of 2018, and about 52% of such reserves is concentrated in the Democratic Republic of Congo. Lithium reserves are concentrated in Chile (more than 57% of global availability), and the world estimated reserves (end 2018) are close to 14,000 thousand tonnes. Rare earth metals and natural graphite reserves are more abundant than lithium and cobalt (respectively, about 117,000 thousand tonnes and 307,000 thousand tonnes, estimated at the end of 2018), and there are large reserves of rare earth metals in China (about 38% of global reserves) [1]. China is recognised as the largest producer, consumer and exporter of rare earth elements (REEs) in the world [2,3]. The concentration of large reserves in one country can lead to price, distribution and sales imbalances. Technologies able to recover these kinds of materials after their use are welcome to reduce the dependence from the producing countries and control the prices.

REEs are considered critical and strategic materials in a wide range of current and innovative applications, causing an important growing in both demand and price of REEs [4–9]. The recycling of rare earths carried out on effluents, waste and scraps generally

consists in the recovery of a single rare earth element or a mixture of rare earths. Electronic waste can be considered a great source of rare earths. Of the 50 million tonnes of WEEE estimated to be disposed of annually in landfills around the world, only about 12.5% is currently recycled for all metals. This type of waste contains high concentrations of rare earth metals as well as metals such as Au, Sn, Ag and Pt [10]. In the case of waste from electrical and electronic equipment (WEEE) containing rare earths in small quantities, the critical step is very often the dismantling of the waste, which is generally carried out by hand despite the numerous attempts by the industry to automate this process for individual types of WEEE. The chemical attack to bring these rare earth elements into a solution is the next step normally performed. Either acid or base attacks are usually adopted, although more complex strategies are also developed, as in the case of the presence of particularly recalcitrant rare earth chemical species. The recovery of rare earths from the fluorescent lamp powder is an example [11–13]. Hydrometallurgy is the main technique used for the separation and purification of rare earths, although other processes are also applied, such as pyrometallurgy [14]. Specifically, the counter-current separation with two immiscible phases, one aqueous containing the rare earths to be separated and the other organic containing the extractant, by using mixer-settler equipment, is an industrial technique used not only for rare earth recycling but also for their industrial production from the minerals. Given the massive environmental impact of hydrometallurgical techniques, numerous studies have been carried out to mitigate them, such as those in which the organic solvent is replaced with an ionic liquid [15–19].

Sprecher et al. [20] studied the production of neodymium and compared the virgin production route of NdFeB magnets with two hypothetical recycling processes in terms of environmental impact. The life cycle assessments, described in this work, indicated that recycling is a promising alternative to conventional production processes. Nevertheless, rare earth recycling is not simple to achieve, which is a challenge for research in the future. Nowadays, the lanthanides are not recycled in large quantities mainly because of low yield and cost; a very high price of feedstock or a government mandate could push towards the development of large-scale recycling processes. End-of-life light-emitting diodes (LED) are electronic waste containing valuable and critical metals such as rare earth elements and gallium. De Oliveira et al. reported the current recovery techniques of LED waste using examples from other e-waste such as fluorescent lamps, liquid crystal displays, and LED production dust [21]. The possible technologies to recover gallium and REE from LED are physical processes, pyrolysis, bioleaching, and acid leaching, followed by purification processes such as solvent extraction and precipitation. Based on this work, hydrometallurgical processing has been identified as the most suitable method to recover gallium and REE from LEDs due to its high efficiency in recovering metals from low-grade secondary raw material. Lorenz and Bertau examined and optimised the solid-state chlorination method for mobilising RE elements from waste streams, in particular from fluorescent lamp scraps and Fe14Nd2B magnets. They found that, without producing strongly acidic wastes and with NH_4Cl as a cheap source for hydrogen chloride, solid-state chlorination provides various advantages in terms of cost and disposal [22]. Becci et al. showed an LCA study on the recovery of REEs from end-of-life permanent magnets, an example of LCA as a support tool for the definition of circular economy strategies for REE recovery [23].

Catalysis also represents an important market for REEs, due to unique properties offered by these materials. In fact, about 20% of REEs are used for catalytic application. It is estimated that about 30,000 tonnes of rare earth oxides, mainly lanthanum and cerium, is used in fluid catalytic cracking (FCC) process and for automobile catalytic converters [2].

The FCC process was established in the last century in order to improve the gasoline production and increase the octane number of the fuel. The FCC feed is normally composed by heavy atmospheric gasoil and light/heavy vacuum distillate, and the catalyst is named USY (ultra-stabilised zeolite Y, FAU-type zeolite). In order to increase the stability, reduce

the coke formation and increase the gasoline and olefin yields, medium-pore zeolite (such as ZSM-5) and/or REE are added to the USY catalyst [24,25].

The FCC catalyst consists of spherical particles in which zeolite crystals are dispersed in amorphous silica-alumina and binders [26–28]. The presence of amorphous silica-alumina allows having large pores that promote mass transfer of heavy molecules in the pellets, improving the efficiency of the catalyst. In the last years, olefins are the most important products from the FCC process, due to their increasing market price. C3 and C4 olefins have multiple application: other than commercialisation, they can used in refineries as feed for alkylation processes and for the production of MTBE and MTPE (methyl tert-butyl ether and methyl tert-pentyl ether, respectively), which are used as high octane number gasoline and anti-knocking agent in gasoline blend.

Olefins are the most important product obtained from an FCC plant; the larger world production is by steam cracking technology, but currently other processes such as MTO-MTH (methanol-to-olefins and methanol-to-hydrocarbons) processes are considered an emergent technologies because in this case it is possible to start from renewable sources [29–32].

The feed of FCC plants contains heavy metals, especially Ni and V, which tend to deposit on the catalyst surface causing poisoning of active sites or hindering diffusion of reactants. Heavy metals also exhibit red-ox catalytic properties, promoting coke formation. Moreover, the doping with rare earth is designed with the aim to have a catalyst able to capture and immobilise the vanadium over REE sites with high capacity and selectivity [33–36]. The presence of rare earths in the FCC catalyst is then fundamental to obtain a catalyst with a significant activity, high selectivity and good stability [37–39].

From these premises, it is then important to develop technologies and processes able to recover strategic materials, such as REEs, from spent FCC catalysts. Although several studies have been performed on the recovery of REEs from batteries, glass scarps and other high-tech devices [40–42], few studies have been published on their retrieval from spent FCC catalysts [43]. In this concern, the aim of this study was to explore the possibility to recover REEs (mainly lanthanum) from fines of industrial FCC catalysts (waste from Petrobras refinery), by using acid leaching and selective separation (the oxalate precipitation method). Different parameters were investigated such as acid type (i.e., HNO_3, HCl and H_2SO_4) and concentration, temperature and time of treatment aiming to optimise the process, in terms of lanthanum recovery and purity. Treated zeolite was also characterised in order to give insights about the effect of leaching on zeolite structure. Zeolite recovery is also an interesting aspect that might be considered in future works.

2. Materials and Methods

The spent FCC catalyst was kindly provided by Fábrica Carioca de Catalisadores S.A. (Rio de Janeiro, Brasil) and the particle size distribution of the as-received sample was measured with Mastersizer2000 (Malvern Instruments). The catalyst was also characterised by X-Ray powder diffraction (APD 2000 Pro) to verify the catalyst structure and zeolite phase, whilst the morphology of the particles was observed on a scanning electron microscope (FEI model Inspect). Textural properties were estimated by nitrogen adsorption–desorption isotherms at 77 K performed with a ASAP 2020 (Micromeritics) instruments. B.E.T. and t-plot methods were adopted for the calculation of surface area and micropore volume, respectively [44]. In order to check the content of the residual coke present in the spent catalyst, thermo-gravimetric analysis was also carried out with a DTG-60 (Shimadzu) instrument, in air flow and by heating the sample from room temperature (RT) to 850 °C (heating rate of 5 °C/min). Inductively coupled plasma optical emission spectrometer (ICP-OES, Perkin Elmer, Optima 8300 model) was also used for chemical analysis.

REE recovering was performed via acid-assisted leaching. For this purpose, analytical grade (Sigma Aldrich) hydrochloric acid (HCl 37%), sulphuric acid (H_2SO_4 96%) and nitric acid (HNO_3 65%) were used, with a maximum acid concentration of 12, 35 and 14 N, respectively. Acid solutions at different concentrations were prepared by dilution

with demineralised water and checked by titration with standard NaOH (Sigma Aldrich) solution. An automatic titrator (Metrohm 905 Titrando) was used to determinate the molar concentration of acidic solution. The acid leaching was performed using 500 mg of exhausted catalyst and 50 mL of acid solution at different concentrations. A thermostatic bath, equipped with an PID thermal controller under stirring, was used to investigate the effect of temperature (in the range 20–80 °C) on the REE recovery process. A water reflux condenser was used to avoid loss of material during the experiments. At the end of the experiment, filtration was performed in order to separate leaching solution from catalyst particles. A selective precipitation of lanthanum, by using a large excess of oxalic acid, was obtained from leaching solutions. ICP-OES was then used for chemical analysis of the liquid filtrate and oxalate metal salts.

3. Results and Discussion

3.1. Characterisation of as Received Sample

The powder XRD pattern of the as received catalyst is reported in Figure 1. Peak analysis indicates FAU-type zeolitic phase as main crystalline phase that may be detected.

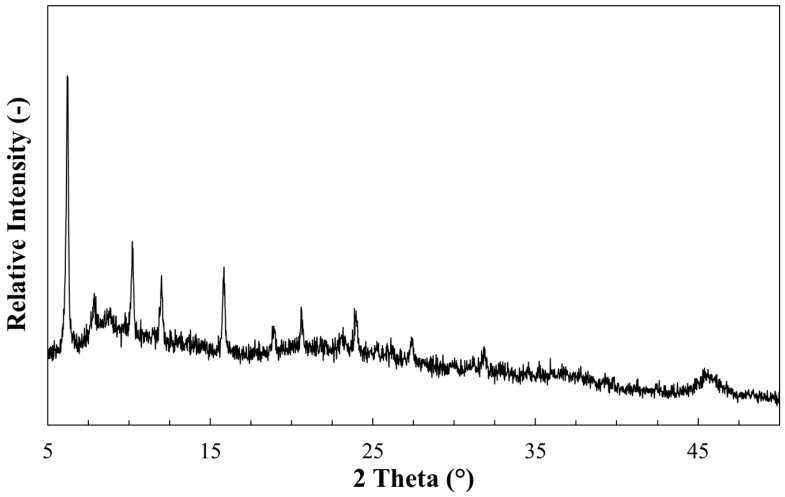

Figure 1. XRD patterns of as received catalyst.

The presence of a slight background in the 20–30° range may be related to the presence of the binder, usually used for the industrial catalyst preparation [44].

Figure 2 shows the particle size distribution, and the profiles clearly indicates that size is in the range 30–300 µm, with a symmetric distribution centred at the value of 104 µm.

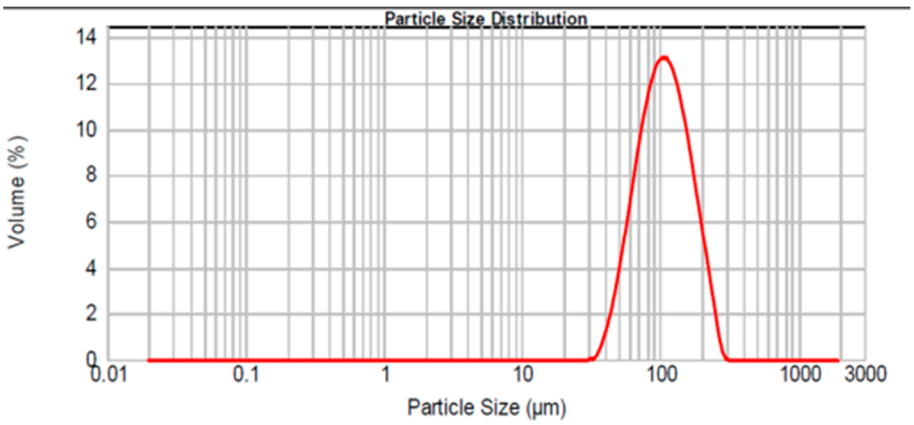

Figure 2. Particle size distribution of as received sample.

The particle size distribution is in accordance with the SEM images reported in Figure 3, where a very uniform size distribution may be noticed.

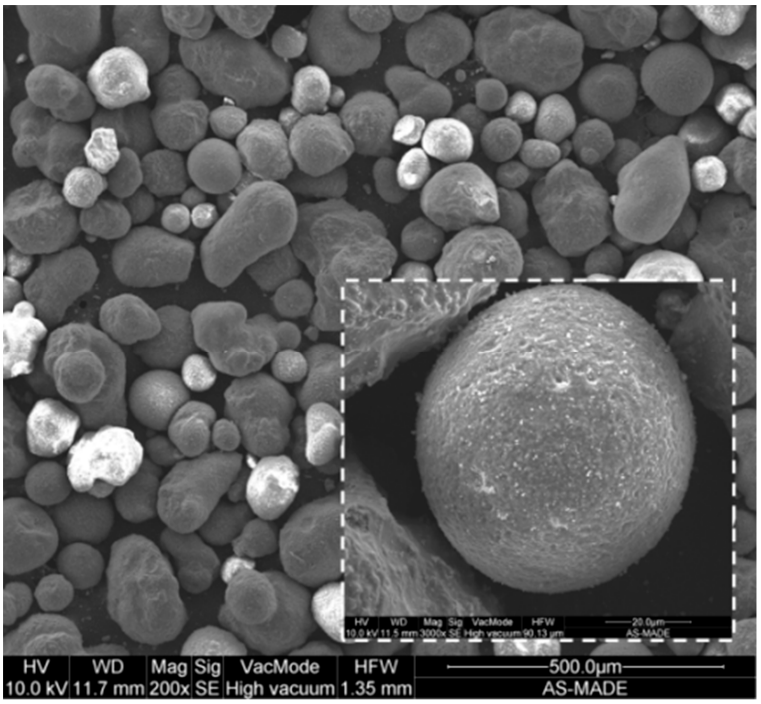

Figure 3. SEM images of as received sample. Magnification in the internal picture.

The SEM images also shows the presence of spherical particles with size below 200 µm, typical of FCC catalyst, with roughness on the external surface due the presence of zeolite crystals [45,46].

The TG/DTA profiles reported in Figure 4 clearly indicate the absence of coke on the investigated samples, as no weight loss is observed above 300 °C [47,48]. The low water content (about 2 wt%), calculated as weight loss in the range of RT-200 °C is typical of hydrophobic materials. In fact, FCC catalyst usually consists of 30–40 wt% of dealuminated FAU-type zeolite and hydrophobic binders (e.g., silica oxides). The absence of coke indicates that the investigated equilibrium catalyst was sampled from the regeneration unit of the FCC plant.

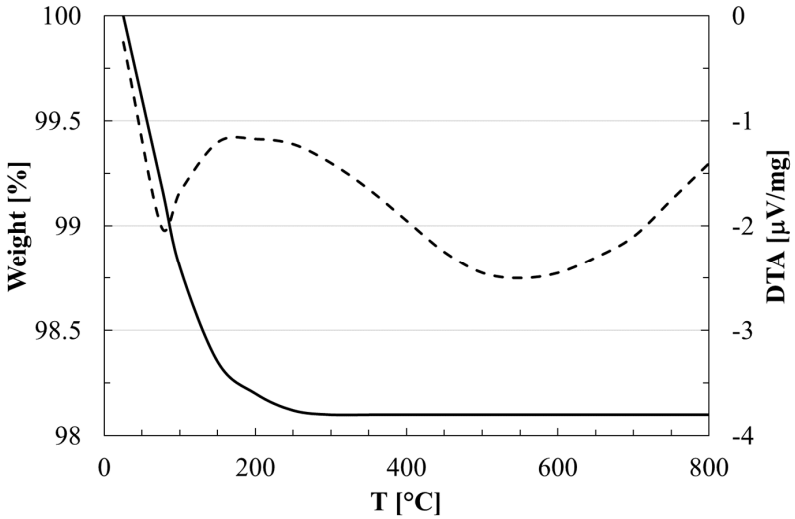

Figure 4. TG/DTA profiles of as-received sample.

Textural and chemical properties of the investigated sample are summarised in Table 1.

Table 1. Physical properties and chemical composition of the investigated FCC sample.

Average particle size (μm) [a]	104
Specific area (m^2/g) [b]	107
Total pore volume (cm^3/g) [c]	0.128
Micropore volume (cm^3/g) [d]	0.039
Mesopore volume (cm^3/g)	0.089
Chemical composition (wt%) [e]	
Al	22.70
La	1.49
Fe	0.74
Ni	0.49
V	0.35
Co	0.0028
Cr	0.0055
Si, O, H, Na	rest of 100%

Calculated: [a] from PSD; [b] from BET; [c] at $P/P^0 = 0.99$; [d] from t-plot; [e] from ICP.

The relatively low both surface area and micropore volume are due to the presence of binders. The mesopore volume is calculated as the difference between total and micropore volume. By considering the pore volume, zeolite content should be about 30% [49].

ICP analysis results reported in Table 1 show a lanthanum content of 1.49 wt%. As already mentioned, this metal is inserted as counter-ion to the zeolite by a post-synthesis ion exchange treatment, and it is active in cracking catalytic reaction [20]. Iron, nickel and vanadium are the most common contaminant metals in exhausted fluid catalytic cracking (FCC) catalysts. In particular, nickel and vanadium are the most relevant poisons for FCC process [50,51]. In fact, the depositing of these metals on the catalyst surface is one of the main causes of catalyst deactivation. Moreover, the presence of such metals favours dehydrogenation reactions leading to a higher coke deposition [26].

3.2. Metals Leaching by Acids: The Effect of Operation Condition on Lanthanum Selectivity

Experimental tests were carried out as previously described using HCl, HNO_3 and H_2SO_4 in different concentration, from 0.1 N to the maximum concentration of commercial acid: 12, 14 and 35 N, respectively. The leaching reaction was performed at 20 °C and atmospheric pressure, for 3 h of contact time. A blank test was performed, by using demineralised water (pH = 7) without acid addition, and no traces of La^{3+} in the aqueous phase were detected, after 3 h of contact time.

Figure 5 shows the recovery of metals ions, calculated as the percentage amount of metal ions leached from the catalyst (aqueous phase) with respect to the total ions amount in the spent catalyst.

The obtained results show that the investigated acids are effective towards lanthanum leaching in the whole investigated acid concentration range, with a maximum recovery of about 60%. At 0.1 N, the recovery of lanthanum is comparable for the different acids: about 35% for both HCl and HNO_3 and 38% for H_2SO_4. When HCl is used, the lanthanum recovery increases up to 60% when increasing the acid concentration to 2 N, and no significant recovery change is observed above this value. On the contrary, for both HNO_3 and H_2SO_4, the maximum lanthanum recovery of about 60% is obtained at 5 and 10 N, respectively, with a decrease observed when further increasing the acid strength.

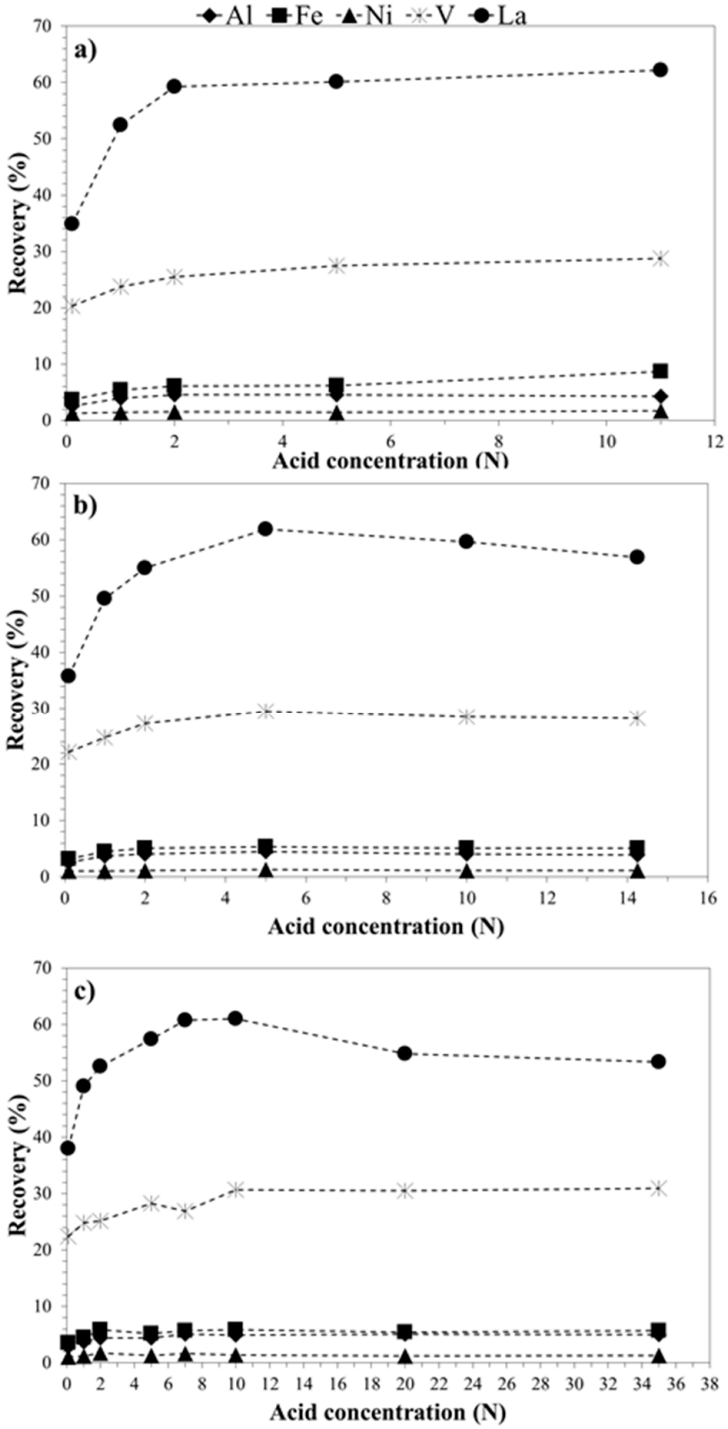

Figure 5. Effect of HCl (**a**), HNO_3 (**b**) and H_2SO_4 (**c**) concentration on metal recovery (test conditions: 20 °C, 3 h).

The investigated acids can also leach vanadium, with a recovery of about 20% at 0.1 N concentration and a maximum of 25–30% for higher concentration. For any other metal, a recovery lower than 10% is measured. In particular, Ni seems to be the most stable against leaching, as the recovery was always lower than 1.5%. The selectivity of leaching process may be defined as follows (Equation (1)):

$$S_i = \frac{Rec_i}{\sum_i Rec_i} \quad (1)$$

where Rec_i is the recovered mass of metal *i*.

Therefore, although the increase of acid concentration seems to favour lanthanum leaching, the lanthanum selectivity is always 0.58 ± 0.02, without any specific effect of acid concentration or acid type.

The effect of temperature on lanthanum recovery was studied for HNO_3 only, since this acid may be preferred in an industrial environment for safety reasons. Furthermore, nitric acid is used during the preparation process of the FCC catalyst, in particular during the dealumination step of the zeolite. Therefore, industries fabricating the FCC catalyst, and that may recycle it for lanthanum recovery, have consolidated technologies and knowledge on the handling of nitric acid. Experimental data reported in Figure 6 show the favourable effect of temperature increase on lanthanum recovery, significant for acid concentrations up to 5 N. In particular, a temperature increase from 20 to 80 °C promotes the lanthanum recovery from ca. 35% to ca. 80% and from ca. 50% to ca. 90%, for acid concentrations of 0.1 and 2 N, respectively. The lanthanum recovery approaches 100% for acid concentration of 5 N at 80 °C. It is indeed well-known that metal leaching is a temperature-favoured phenomenon [52].

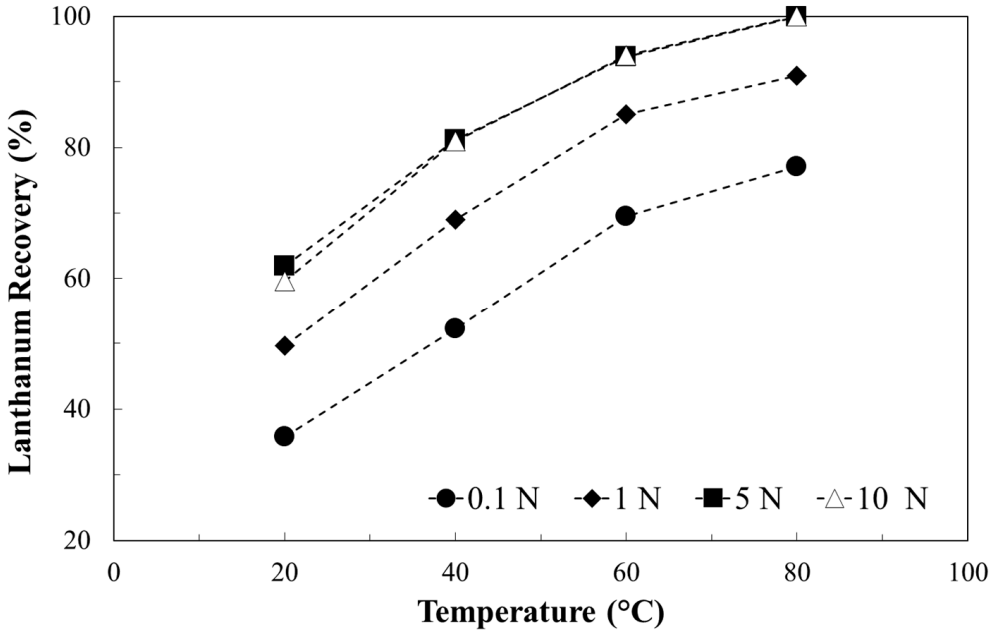

Figure 6. Effect of temperature and HNO_3 concentration on lanthanum recovery (time tests: 3 h).

However, a similar effect is also observed for the other elements, as reported in Table 2. For 5 N HNO_3 concentration, aluminium leaching increases from 4.5% to 21.7% by increasing the temperature from 20 to 80 °C. However, it should be considered that the increase in aluminium concentration in the liquid phase can also derive from the zeolite framework dealumination, a well-known phenomenon favoured by acids at high temperature [53,54].

Similar trends are observed for Fe, Ni and V. In particular, Fe recovery increases up to 24.4% and V recovery up to 43%. Ni is confirmed to be the most stable element, since only 6.3% is recovered at 80 °C.

Figure 7 shows that lanthanum selectivity (as defined above) exhibits a volcano trend with temperature, with an optimal temperature depending on the acid concentration. For acid concentrations equal to 0.1 N, lanthanum recovery selectivity increases from 0.55 to 0.60 by increasing the temperature from 20 to 80 °C. On the contrary, for higher acid concentrations, the maximum in selectivity is reached at 40 °C, with a value above 0.6. For acid concentrations equal to 5 N, by increasing the temperature from 40 to

80 °C, lanthanum selectivity drops from 0.63 to 0.51, which can mainly be attributed to a mass extraction of Al and Fe higher than the lanthanum one.

Table 2. Effect of temperature and HNO_3 concentration on metals recovery.

Temperature (°C)	[HNO_3] (N)	Al (%)	Fe (%)	Ni (%)	V (%)
20 °C	0.1	2.6	3.2	1.0	22.1
	1	3.7	4.5	1.1	24.7
	2	4.0	5.1	1.1	27.2
	5	4.5	5.4	1.3	29.5
	10	4.0	5.1	1.2	28.4
40 °C	0.1	4.6	5.4	1.6	24.2
	1	5.8	6.6	1.8	28.1
	2	6.1	7.0	1.9	29.1
	5	6.5	7.9	1.9	31.8
	10	6.5	7.9	2.0	32.3
60 °C	0.1	7.6	7.8	2.3	28.3
	1	9.3	10.4	2.7	30.1
	2	9.6	11.2	2.7	32.4
	5	10.9	13.3	3.1	33.8
	10	10.8	13.3	3.1	35.5
80 °C	0.1	10.5	9.9	2.9	27.9
	1	15.1	16.5	4.3	34.5
	2	18.0	19.6	5.0	37.3
	5	21.7	24.4	6.3	43.0
	10	19.6	24.4	6.2	41.6

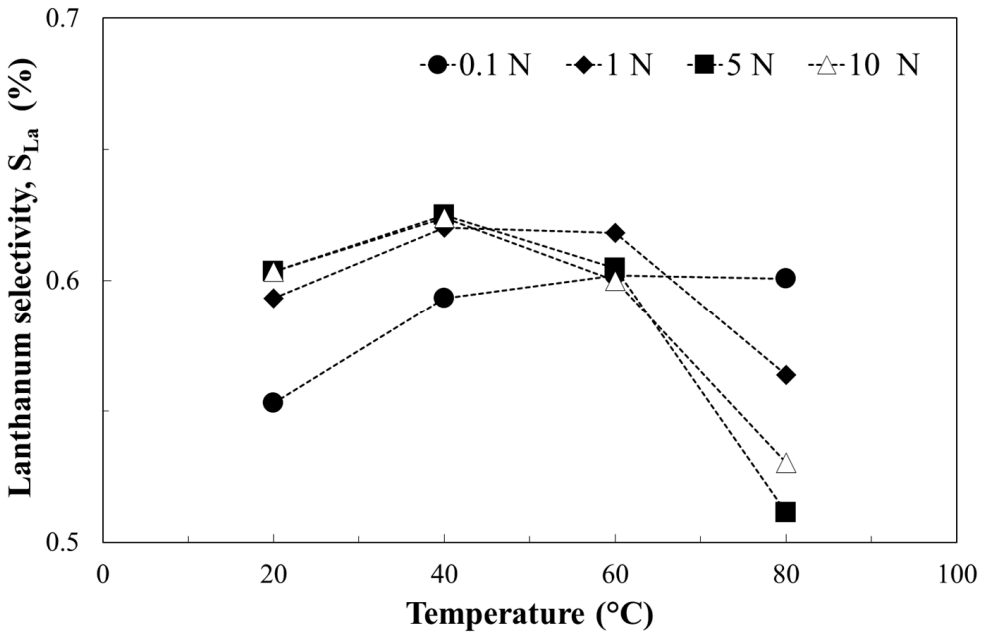

Figure 7. Effect of temperature and HNO_3 concentration on lanthanum selectivity (time tests: 3 h).

In order to check the effect of contact time on the metal recovery, HNO_3 5 N solution was used in the process time range 2–300 min. As expected (Figure 8), the obtained results show that the recovery of all metals increases with time, reaching a plateau after 3 h. Due to the differences between metals in leaching over time, the mass concentration of the recovered metals also changes with time.

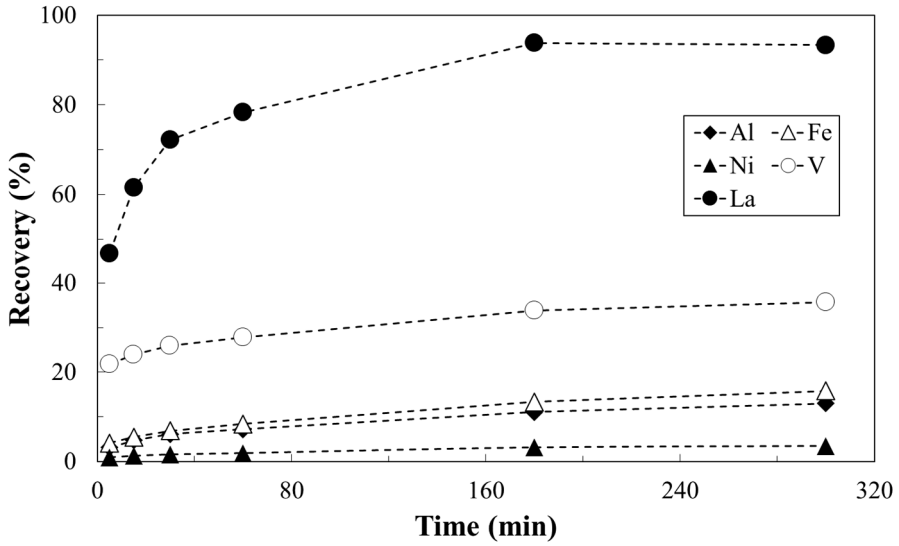

Figure 8. Effect of contact time on metal recovery. (test conditions: HNO_3 5 N, 60 °C).

Figure 9 reports the relative weight fraction of metals (W_i) calculated as follows (Equation (2)):

$$W_i = \frac{[M]_i}{\sum_i [M]_i} \cdot 100 \quad (2)$$

where $[M]_i$ is the concentration of metal i (expressed in mg/L) in the liquor.

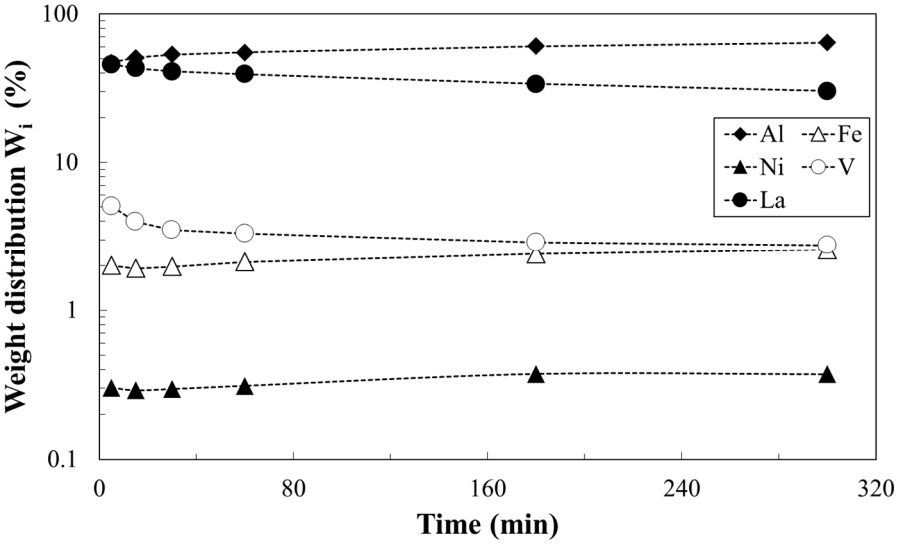

Figure 9. Effect of contact time on metal distribution recovery (test conditions: HNO_3 5 N, 60 °C).

As reported in Figure 9, W_{La} decreases from about 45 wt% to about 30 wt% by increasing the treatment time from 15 min to 3 h. This is mainly due to the aluminium extraction also coming out from the zeolite framework as explained above.

With the above-discussed tests, it is only possible to recover an aluminium-rich solution; therefore, if pure lanthanum is the target, a second step of purification should be considered. In this concern, in order to recover the extracted lanthanum from the solution, a selective precipitation in oxalic acid was performed. A mother acid solution was prepared, using nitrate salts of La, Al, V, Ni and Fe, with the same metal ion mass fractions of the test with [HNO_3] = 5 N, T = 60 °C and t = 3 h. By using an excess of oxalic acid, the metals are selectively precipitated as oxalates, and the distribution of recovered metals is reported

in Table 3. From the reported data, it clearly appears that lanthanum is 96.3% in mass of the precipitated metals, and the yield of La recovered from the acid solution after the secondary precipitation approaches 100%. It is noteworthy that, even though the initial solution is rich in aluminium, the final concentration of this metal is below 0.034, indicating a good selectivity toward lanthanum of the oxalate precipitation method. In addition, other metals, poisonous for the FCC process (Ni, V), account for a total mass fraction of 0.0022 of the precipitated solid.

Table 3. Metal composition of recovered powder after oxalic acid precipitation.

La wt%	Al wt%	Fe wt%	V wt%	Ni wt%
96.3	3.33	0.13	0.22	0.02

The results clearly show that the adopted precipitation procedure is highly effective and selective towards lanthanum recovery and purification. It is worth noticing that the neglectable amount of poisoning species from the treated refinery cut makes the recovered lanthanum oxalate recyclable for addition to fresh FCC catalyst.

In addition, as mentioned before, the presence of aluminium in the leaching solution is due to a partial dealumination of the catalyst framework [55], even though the treatment does not compromise the zeolite structure, as may be observed from the XRD patterns of the solid phase recovered after acid attack in Figure 10.

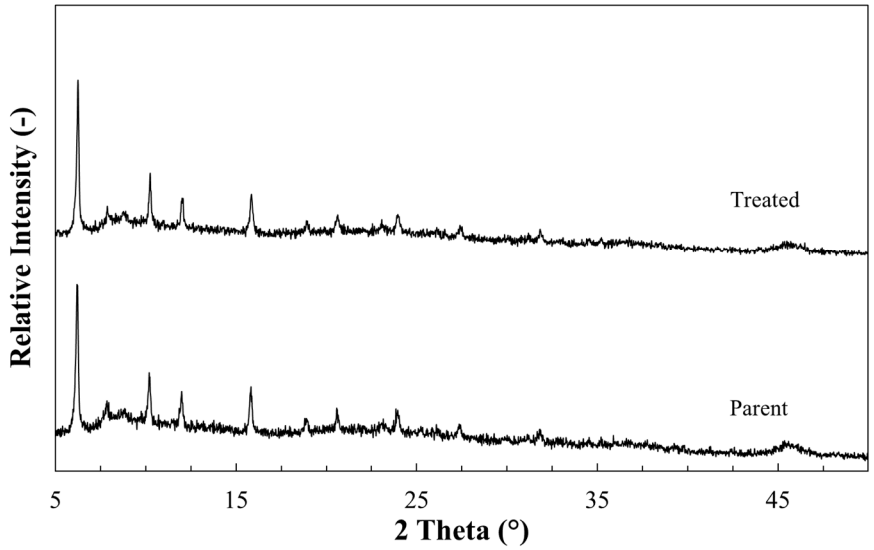

Figure 10. XRD pattern of parent sample and sample treated with HNO_3 5 N (60 °C, 3 h).

The relative intensity of the peak is not affected by acid treatment, suggesting that no significant change in crystalline structure occurs upon treatment.

Contrariwise, the acid treatment causes some change in textural properties. Figure 11 reports a comparison between parent and treated samples of N_2 adsorption–desorption isotherms, showing that the amount of adsorbed N_2 by the treated sample is higher than the parent catalyst, at any relative pressure. Because of the acid treatment, the B.E.T. surface area increases from 107 to 141 m^2/g, while micropore volume decreases from 0.039 to 0.033 cm^3/g. Furthermore, the mesopore volume (calculated as the difference between total pore volume at $P/P^\circ = 0.99$ and micropore volume) increases from 0.089 to 0.131 cm^3/g. The mesopore volume increase may be associated to both metal leaching from the zeolite framework (mainly aluminium [56]) and potential binder dissolution. Figure 11 also reports the pore size distribution of treated and parent samples, confirming the increase in

mesopores as a consequence of the acid treatment. This evidence is also supported by the SEM analysis of the treated sample (Figure 12), as the presence of roughness is clear on the external surface of the particle, coherently with the measured mesopores.

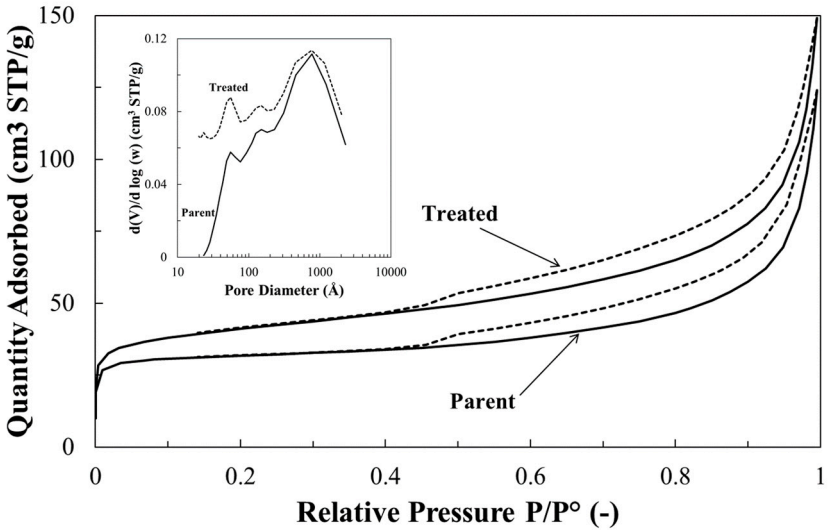

Figure 11. N_2 adsorption (continuous line) and desorption (dashed line) isotherms at 77 K of parent sample and sample treated with HNO_3 5 N, at 60 °C for 3 h. Pore size distribution in the inset.

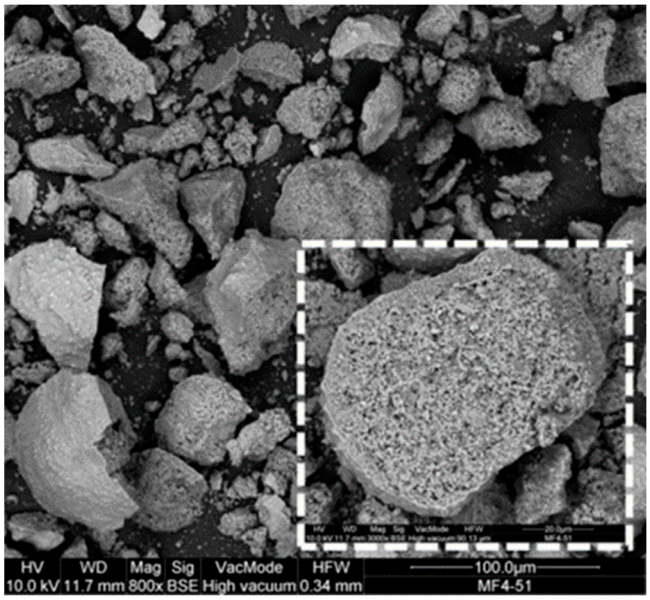

Figure 12. SEM images of sample treated with HNO_3 5 N, at 60 °C for 3 h. Magnification in the inset.

4. Conclusions

In this study, the rare earth element recovery from spent FCC catalyst via acid leaching was investigated. Aiming at investigating a combined acid-leaching/oxalate precipitation process, hydrochloric, sulphuric and nitric acids were tested for the extraction step. Different acid concentrations were used, and the data show that the leaching process depends on acid solution strength with an optimal concentration around 5 M. Any further increase in the acid molarity did not impact on the leaching efficiency, whatever the acid type. For this reason, the assessment of the other process parameters was performed by using only nitric acid, which is less dangerous than the other two when handled in an industrial environment. Temperature increase from 20 to 80 °C favourably impact on the lanthanum recovery from the solid, even though the selectivity toward this metal decreases above

60° as a consequence of a more effective aluminium leaching from the zeolite structure. As for the contact time in batch experiment, it was demonstrated that short contact time (corresponding to a reduced number of equilibrium stages in an industrial extraction plant) did not allow the complete recovery of the REE that takes place only after 3 h of treatment, also enhancing the phenomenon of aluminium leaching. Oxalate salt precipitation was investigated as purification step of the metal ion-rich solution, and a precipitated solid that contains more than 96% of lanthanum was obtained, the rest being essentially aluminium. The neglectable amount of other metals (such as Va and Ni, poisonous for the catalyst) suggests that the recovered REE could be recycled to dope fresh FCC catalyst. As a general point, even though the price of REEs has been very fluctuating over the last decades, in view of a further increase in the demand of such metals for new widespread applications, the suggested separation/purification method could represent a reliable alternative to reuse lanthanum, reducing the potential economic damage from price increases of this REE.

Author Contributions: Conceptualisation, C.S. and M.M. (Massimo Migliori); methodology, M.M. (Massimo Morgana) and A.B.; investigation, M.F. and A.R.; data curation, C.S. and E.C.; writing—original draft preparation, E.C.; writing—review and editing, M.M. (Massimo Migliori) and M.M. (Massimo Morgana); supervision, G.B. and G.G. All authors have read and agreed to the published version of the manuscript.

Funding: This research received no external funding.

Institutional Review Board Statement: Not applicable.

Informed Consent Statement: Not applicable.

Conflicts of Interest: The authors declare no conflict of interest.

References

1. BP Statistical Review of World Energy. 2019. Available online: https://www.bp.com/content/dam/bp/business-sites/en/global/corporate/pdfs/energy-economics/statistical-review/bp-stats-review-2019-full-report.pdf (accessed on 8 July 2020).
2. Blasi, A.; Sposato, C.; Devincenzis, G.; Garzone, P.; Morgana, M. Definition of the Process to Separate Light Rare Earths by Working with (2-Ethylexyl)-Mono(2-Ethylexyl)ester Phosphonic Acid (P507) in a Mixer Settler Battery. In Proceedings of the TMS Annual Meeting, San Diego, CA, USA, 16–20 February 2014; Volume 197.
3. Macheri, N.A.; Sprecher, B.; Bailey, G.; Ge, J.; Tukker, A. Effect of Chinese policies on rare earth supply chain resilience. *Resour. Conserv. Recycl.* **2019**, *142*, 101. [CrossRef]
4. Bezzina, J.P.; Ogden, M.D.; Moon, E.M.; Soldenhoff, K.L. REE behavior and sorption on weak acid resins from buffered media. *J. Ind. Eng. Chem.* **2018**, *59*, 440. [CrossRef]
5. Baniasadi, M.; Vakilchap, F.; Bahaloo-Horeh, N.; Mousavi, S.M.; Fernaud, S. Advances in bioleaching as a sustainable method for metal recovery from e-waste: A review. *J. Ind. Eng. Chem.* **2019**, *76*, 75–90. [CrossRef]
6. Sposato, C.; Blasi, A.; Romanelli, A.; Braccio, G.; Morgana, M. Behavior of sec-octylphenoxy acetic acid (CA-12) in yttrium recovery from high concentrated heavy rare earths mixture. In *Rare Metal Technology*; Springer: Cham, Switzerland, 2017; pp. 225–233.
7. Blasi, A.; Sposato, C.; Romanelli, A.; Braccio, G.; Morgana, M. Study of a synergistic solvent extracting system to separate yttrium and heavy rare earths: A deep investigation on system behavior. In *Rare Metal Technology*; Springer: Cham, Switzerland, 2017; pp. 277–284.
8. Sposato, C.; Blasi, A.; Devincenzis, G.; Garzone, P.; Morgana, M. Comparison among different extractants, AS (2-ethylhexyl)-mono (2-ethylhexyl) ester phosphonic acid (p507), secondary-octyl phenoxy acetic acid (CA-12) and BIS(2, 4, 4-trimethylpentyl)phosphinic acid (CYANEX272), in the separation of heavy rare earths via hydrometallurgical processes. In Proceedings of the TMS Annual Meeting, San Diego, CA, USA, 16–20 February 2014; Volume 201.
9. Molino, A.; Giordano, G.; Motola, V.; Fiorenza, G.; Nanna, F.; Braccio, G. Electrciity production by biomass steam gasification using a high efficiency technology and low environmental impact. *Fuel* **2013**, *103*, 179–192. [CrossRef]
10. Balaram, V. Rare earth elements: A review of applications, occurrence, exploration, analysis, recycling, and environmental impact. *Geosci. Front.* **2019**, *10*, 1285–1303. [CrossRef]
11. Binnemans, K.; Jones, P.T. Perspectives for the recovery of rare earths from end-of-life fluorescent lamps. *J. Rare Earths* **2014**, *32*, 195–200. [CrossRef]
12. Yurramendi, L.; Gijsemans, L.; Forte, F.; Aldana, J.L.; del Rio, C.; Binnemans, K. Enhancing rare-earth recovery from lamp phosphor waste. *Hydrometallurgy* **2019**, *187*, 38–44. [CrossRef]
13. Huckenbeck, T.; Otto, R.; Haucke, E.; Osram, A.G. Verfahren zur Rückgewinnung Seltener Erden aus Leuchtstofflampen Sowie Zugehörige Leuchtstoffe und Lichtquellen. WO2012143240 A2, 26 October 2012.

14. Sun, T.; Kennedy, M.W.; Yurramendi, L.; Aldana, J.L.; Del Rio, C.; Arnout, S.; Trannel, G.; Aune, R.E. Pyrometallurgical Treatment of Apatite Concentrate with the Objective of Rare Earth Element Extraction: Part I. *J. Sustain. Metall.* **2017**, *3*, 829–845. [CrossRef]
15. Prusty, S.; Pradhan, S.; Mishra, S. Ionic liquid as an emerging alternative for the separation and recovery of Nd, Sm and Eu using solvent extraction technique—A review. *Sustain. Chem. Pharm.* **2021**, *21*, 100434.
16. Hidayah, N.N.; Abidin, S.Z. The evolution of mineral processing in extraction of rare earth elements using liquid-liquid extraction: A review. *Miner. Eng.* **2018**, *121*, 146–157. [CrossRef]
17. Hammache, Z.; Bensaadi, S.; Berbar, Y.; Audebrand, N.; Szymczyk, A.; Amara, M. Recovery of rare earth elements from electronic waste by diffusion dialysis. *Sep. Purif. Technol.* **2021**, *254*, 117641. [CrossRef]
18. Arrachart, G.; Couturier, J.; Dourdain, S.; Levard, C.; Pellet-Rostaining, S. Recovery of rare earth (REEs) using ionic solvents. *Processes* **2021**, *9*, 1202. [CrossRef]
19. Zinoveev, D.; Pasechnik, L.; Fedotov, M.; Dyubanov, V.; Grudinsky, P.; Alpatov, A. Extraction of valuable elements from red mud with focus on using liquid media—A review. *Processes* **2021**, *6*, 38.
20. Wang, K.; Adidharma, H.; Radosz, M.; Wan, P.; Xu, X.; Russell, C.K.; Tian, H.; Fan, M.; Yu, J. Recovery of rare earth elements with ionic liquids. *Green Chem.* **2017**, *19*, 4469–4493. [CrossRef]
21. de Oliveira, R.P.; Benvenuti, J.; Espinosa, D.C.R. A review of the current progress in recycling technologies for gallium and rare earth elements from light-emitting diodes. *Renew. Sustain. Energy Rev.* **2021**, *145*, 111090. [CrossRef]
22. Becci, A.; Beolchini, F.; Amato, A. Sustainable strategies for the exploitation of End-of-Life permanent magnets. *Processes* **2021**, *9*, 857. [CrossRef]
23. Lorenz, T.; Bertau, M. Recycling of Rare Earth Elements. *Phys. Sci. Rev.* **2017**, *2*, 20160067. [CrossRef]
24. Adewuyi, Y.G.; Klocke, D.J.; Buchanan, J.S. Effects of high-level additions of ZSM-5 to a fluid catalytic cracking (FCC) RE-USY catalyst. *Appl. Catal. Gen.* **1995**, *131*, 121. [CrossRef]
25. Degnan, T.F.; Chitnis, G.K.; Schipper, P.H. History of ZSM-5 fluid catalytic cracking additive development at Mobil. *Microporous Mesoporous Mater.* **2000**, *35*, 245. [CrossRef]
26. Ibarra, A.; Hita, I.; Azkoiti, M.J.; Arandes, J.M.; Bilbao, J. Catalytic cracking of raw bio-oil under FCC unit conditions over different zeolite-based catalysts. *J. Ind. Eng. Chem.* **2019**, *75*, 372. [CrossRef]
27. Harding, R.H.; Peters, A.W.; Nee, J.R.D. New developments in FCC catalyst technology. *Appl. Catal. Gen.* **2001**, *221*, 389. [CrossRef]
28. Rawlence, D.J.; Gosling, K. FCC catalyst performance evaluation. *Appl. Catal.* **1988**, *43*, 213. [CrossRef]
29. Catizzone, E.; Cirelli, Z.; Aloise, A.; Lanzafame, P.; Migliori, M.; Giordano, G. Methanol conversion over ZSM-12, ZSM-22 and EU-1 zeolites: From DME to hydrocarbons production. *Catal. Today* **2018**, *304*, 39. [CrossRef]
30. Palčić, A.; Catizzone, E. Application of nanosized zeolites in methanol conversion processes: A short review. *Curr. Opin. Green Sustain. Chem.* **2021**, *27*, 100393. [CrossRef]
31. Catizzone, E.; van Daele, S.; Bianco, M.; Di Michele, A.; Aloise, A.; Migliori, M.; Valtchev, V.; Giordano, G. Catalytic application of ferrierite nanocrystals in vapour-phase dehydration of methanol to dimethyl ether. *Appl. Catal. B Environ.* **2019**, *243*, 273. [CrossRef]
32. Tian, P.; Wei, Y.; Ye, M.; Liu, Z. Methanol to olefins (MTO): From fundamentals to commercialization. *ACS Catal.* **2015**, *5*, 1922. [CrossRef]
33. Escobar, A.S.; Pereira, M.M.; Pimenta, R.D.M.; Lau, L.Y.; Cerqueira, H.S. Interaction between Ni and V with USHY and rare earth HY zeolite during hydrothermal deactivation. *Appl. Catal. Gen.* **2005**, *286*, 196. [CrossRef]
34. Zhang, W.; Guo, Y.; Gong, X.; Guo, Y.; Wang, Y.; Lu, G. Current status and perspectives of rare earth catalytic materials and catalysis. *J. Catal.* **2014**, *35*, 1238.
35. Xiaoning, W.; Zhen, Z.; Chunming, X.; Aijun, D.; Li, Z.; Guiyuan, J. Effects of light rare earth on acidity and catalytic performance of HZSM-5 zeolite for catalytic cracking of butane to light olefins. *J. Rare Earth* **2007**, *25*, 321. [CrossRef]
36. Falabella, E.; Trigueiro, F.E.; Zotin, F.M.Z. The role of rare earth elements in zeolites and cracking catalysts. *Catal. Today* **2013**, *115*, 218–219.
37. De la Puente, G.; Falabella, E.; Zotin, F.M.Z.; Camorim, V.L.D.; Sedran, U. Influence of different rare earth ions on hydrogen transfer over Y zeolite. *Appl. Catal. Gen.* **2000**, *197*, 41. [CrossRef]
38. Sterte, J.; Otterstedt, J.E. Catalytic cracking of heavy oil: Use of alumina—montmorillonites both as catalysts and as matrices for rare earth exchanged zeolite Y molecular sieve. *Appl. Catal.* **1988**, *38*, 131. [CrossRef]
39. Scherzer, J. Designing FCC catalysts with high-silica Y zeolites. *Appl. Catal.* **1991**, *75*, 1. [CrossRef]
40. Jha, M.K.; Kumari, A.; Panda, R.; Kumar, J.R.; Yoo, K.; Lee, J.Y. Review on hydrometallurgical recovery of rare earth metals. *Hydrometallurgy* **2016**, *165*, 2. [CrossRef]
41. Binnemans, K.; Jones, P.T.; Blanpain, B.; Van Gerven, T.; Pontikes, Y. Towards zero-waste valorisation of rare-earth-containing industrial process residues: A critical review. *J. Clean. Prod.* **2015**, *99*, 17. [CrossRef]
42. Shengqiang, Z.; Xiuyang, H.; Dahui, W. Review on comprehensive recovery of valuable metals from spent electrode materials of nickel-hydrogen batteries. *Rare Metal Mater. Eng.* **2015**, *44*, 73. [CrossRef]
43. Innocenzi, V.; Ferella, F.; De Michelis, I.; Vegliò, F. Treatment of fluid catalytic cracking spent catalysts to recover lanthanum and cerium: Comparison between selective precipitation and solvent extraction. *J. Ind. Eng. Chem.* **2015**, *24*, 92. [CrossRef]

44. Lanzafame, P.; Papanikolaou, G.; Perathoner, S.; Centi, G.; Migliori, M.; Catizzone, E.; Giordano, G. Reassembly mechanism in Fe-Silicalite during NH4OH post-treatment and relation with acidity and catalytic reactivity. *Appl. Catal. Gen.* **2019**, *508*, 186–196. [CrossRef]
45. Woltermann, G.M.; Magee, J.S.; Griffith, S.D. Chapter 4 Commercial Preparation and Characterization of FCC Catalysts. *Stud. Surf. Sci. Catal.* **1993**, *76*, 105–144.
46. Gonzalez, M.R.; Pereyra, A.M.; Torres Sánchez, R.M.; Basaldella, E.I. Chromium removal by zeolite-rich materials obtained from an exhausted FCC catalyst: Influence of chromium incorporation on the sorbent structure. *J. Colloid Interf. Sci.* **2013**, *408*, 21–24. [CrossRef] [PubMed]
47. Behera, B.; Gupta, P.; Ray, S.S. Structure and composition of hard coke deposited on industrial fluid catalytic cracking catalysts by solid state 13C nuclear magnetic resonance. *Appl. Catal. Gen.* **2013**, *466*, 123–130. [CrossRef]
48. Migliori, M.; Catizzone, E.; Aloise, A.; Bonura, G.; Gómez-Hortigüela, L.; Frusteri, L.; Cannilla, C.; Frusteri, F.; Giordano, G. New insights about coke deposition in methanol-to-DME reaction over MOR-, MFI-and FER-type zeolites. *J. Ind. Eng Chem.* **2018**, *68*, 196. [CrossRef]
49. Tonnetto, G.; Atias, J.; De Lasa, H. FCC catalysts with different zeolite crystallite sizes: Acidity, structural properties and reactivity. *Appl. Catal. Gen.* **2004**, *270*, 9–25. [CrossRef]
50. Escobar, A.S.; Pinto, F.V.; Cerqueira, H.S.; Pereira, M.M. Role of nickel and vanadium over USY and RE-USY coke formation. *Appl. Catal. A* **2006**, *315*, 68–73. [CrossRef]
51. Roncolatto, R.E.; Cardoso, M.J.B.; Cerqueira, H.S.; Lam, Y.L.; Schmal, M. XPS study of spent FCC catalyst regenerated under different conditions. *Ind. Eng. Chem. Res.* **2007**, *46*, 1148–1152. [CrossRef]
52. Seader, J.D.; Henley, E.J.; Roper, D.H. *Separation Process Principles*, 3rd ed.; John Wiley & Sons, Inc.: Hoboken, NJ, USA, 2011.
53. Giudici, R.; Kouwenhoven, H.W.; Prins, R. Comparison of nitric and oxalic acid in the dealumination of mordenite. *Appl. Catal. Gen.* **2000**, *203*, 101–110. [CrossRef]
54. Mintova, S.; Valtchev, V.; Onfroy, T.; Marichal, C.; Knözinger, H.; Bein, T. Variation of the Si/Al ratio in nanosized zeolite Beta crystals. *Microporous Mesoporous Mater.* **2006**, *90*, 237–245. [CrossRef]
55. Gao, X.; Owens, W.T. Process for Metal Recovery from Catalyst Waste. U.S. Patent 2012/0156116 A1, 21 June 2012.
56. Disegna, W.L.; Foster, R.L. Catalyst Demetallization. U.S. Patent 3252918, 24 May 1966.